Int J Adv Manuf Technol (2014) 73:773–782
DOI 10.1007/s00170-014-5865-9

ORIGINAL ARTICLE

Time-varying positioning error modeling and compensation for ball screw systems based on simulation and experimental analysis

Zihan Li · Kaiguo Fan · Jianguo Yang · Yi Zhang

Received: 6 September 2013 / Accepted: 11 April 2014 / Published online: 8 May 2014

Abstract Thermal expansion of ball screw systems affects the machining accuracy of machine tools significantly. This paper intends to provide a comprehensive error compensation method for the time-varying positioning error of machine tools. To confirm the thermal deformation mechanism of ball screw systems, experiments have been designed to study the thermal behaviors of a ball screw system under varying temperature conditions. An exponential algorithm is proposed to predict the temperature variation pattern of the ball screw based on finite element analysis, and the actual thermal boundary conditions of the ball screw system are exactly defined according to the proposed algorithm and the experimental results. Then, a comprehensive compensation model is established based on the decomposition of the initial geometric error and thermal error components. Finally, a real-time error compensation system is developed for machine tools based on the function of external machine original coordinate shift and fast Ethernet data interaction, and satisfactory results have been achieved for the compensation experiments on a machining center.

Keywords Machine tools · Time-varying positioning error · Thermal error · Error compensation · Finite element analysis

1 Introduction

Ball screw systems are widely used in machine tools to convert rotational motion into linear motion. However, a ball screw generates lots of friction heat at the contact areas, such as the ball nut and the supporting bearings, which would result in great thermal deformation along the ball screw shaft. It has been confirmed that thermal errors severely affect the machine tool accuracy, as they account for 40–70 % of the total errors [1, 2]. Therefore, thermal deformation of ball screw systems is one of the most important issues to consider for high-precision machine tools.

There are generally two methods to deal with machine tool errors: error control and error compensation [3]. Thermally symmetric design of machine structure, air-cooling system with a hollow ball screw, room temperature-controlled workshop, adjustable preload for the supporting bearings, etc. [4, 5] are the generally used methods to control machine tool errors. However, the methods mentioned above can only minimize the thermal errors to some degree with great cost. While error compensation has been confirmed to be one of the most efficient and cost-effective methods to improve machine tool accuracy [6].

An error model with high accuracy and robustness is the key factor for error compensation. Yang et al. [7] applied a novel data processing method to optimize the temperature variables, and then a robust mathematical model was developed for a turning center. Wu et al. [8] introduced a comprehensive multiple regression method to study the relationship between temperature variation and thermal error for a ball screw system. Wang et al. [9] proposed a compound error model for the geometric and thermal errors of a milling center based on Newton interpolation. Besides, many other methods were also proposed to map the temperature data to the thermal errors, such as neural network [10–13], time series model [14, 15], gray model [16, 17], and support vector model [18]. In general, the majority of the work done above has concentrated on the study of the relationship between thermal error and key heat source temperature from different perspectives. While for a ball screw, there usually exists inconsistency between its temperature field and the key heat source temperature under varying thermal states, so it is hard to maintain the accuracy

Z. Li (✉) · K. Fan · J. Yang · Y. Zhang
School of Mechanical Engineering, Shanghai Jiao Tong University, Shanghai 200240, China
e-mail: lizihan123@sjtu.edu.cn

and robustness of the compensation model in the actual application.

To resolve this problem, other researchers have tried to study thermal errors from the thermal deformation mechanism of machine tools. Ko et al. [19] investigated the thermal bending behavior of a spindle simplified as a simple beam. Kim et al. [20] analyzed the temperature distribution along a ball screw system using finite element method (FEM) with bilinear type. Xia et al. [21] conducted a series of tests to estimate the dynamic characteristics of a ball screw system. Min et al. [22] proposed to simulate the thermally induced deformation of a ball screw system based on finite element model. Though the temperature rising pattern is similar between the simulation and the experimental results, their absolute values still exist some significant deviation, which is attributed to the fact that it is difficult to establish the accurate thermal boundary conditions for the ball screw system just according to the conventional empirical formula.

This paper intends to provide a comprehensive error compensation method for the time-varying positioning error of machine tools based on simulation and experimental analysis. In the next section, experiments have been designed to study the thermal behaviors of a ball screw system under varying temperature conditions. Then, the thermal analysis of the ball screw temperature field and the modeling process for the time-varying positioning error are presented in Sections 3 and 4, respectively. Finally, a novel error compensation method is introduced in Section 5, and compensation experiments were conducted on a machining center to verify the effectiveness of the real-time error compensation system.

2 Experimental setup and measurement results

2.1 Experimental setup and procedure

To study the thermal deformation mechanism of ball screw systems, an experiment was carried out on the *X*-axis ball screw of a vertical machining center. The parameters of the ball screw are shown in Table 1.

In order to measure the temperature of the ball screw, a portable wireless temperature sensor with high measuring precision of 0.1 °C and fast response characteristic was specially developed. It could be attached to the ball screw surface with its magnetic base and read the temperature data in a short time, and then quickly removed after collecting the required data. Six wireless temperature sensors were arranged along the *X*-axis stroke range evenly as shown in Fig. 1, and an additional wireless temperature sensor was used to monitor the variation of the ambient temperature.

According to the measuring criterion of ISO230-2 [23] and ISO230-3 [24], a laser interferometer was used to measure the *X*-axis positioning error. The machine reference origin was set to be the starting point for this measurement, and the positioning error was measured every 80 mm in the whole stroke range of 800 mm. To detect the thermal error, the positioning error was measured under different temperature conditions. Firstly, the initial geometric error was measured at normal temperature when the machine tool was initially switched on. And then, the machine tool was warmed up by moving the *X*-axis slide along its stroke range with a feed rate of 8 m/min. Meanwhile, the temperature measurement was taken at an interval of 10 min until the ball screw system reached a thermal equilibrium state. And the positioning error was measured synchronously after the machine tool had been warmed up for 10, 20, 30, 40, 60, 80, 100, and 120 min, respectively.

Thereafter, in order to simulate the actual working process, the machine tool was stopped to study the thermal behaviors during the natural cooldown phase. Since the temperature of the ball screw dropped dramatically in the initial period and gradually slowed down until a steady state, the temperature measurement was taken at an interval of 5 min in the first 30 min and then at an interval of 10 min in the next 60 min. Meanwhile, the positioning error was measured synchronously after the machine tool had been cooled down for 5, 10, 20, 30, 40, 50, and 70 min, respectively.

Table 1 Parameters of the ball screw

Parameters	Value
Diameter	40 mm
Pitch	16 mm
Stroke range	800 mm
Maximum feed rate	20 m/min
Length between two bearings	900 mm

2.2 Experimental results and discussion

Figure 2 shows the temperature variation of the six measurement points on the ball screw. It can be seen from Fig. 2 that the temperature variation in the middle part of the ball screw is almost the same, T_{bs1} and T_{bs6} are a little lower, but the deviation between the six measurement points is quite small. This observation could be explained as follows: owing to the preload and complex kinematics of the recirculating nut, the largest portion of the friction heat was generated by the moving nut, and the ball screw was warmed up evenly over its whole stroke range. So, the average temperature of the ball screw (as defined in Eq. (1)) can be used to represent the

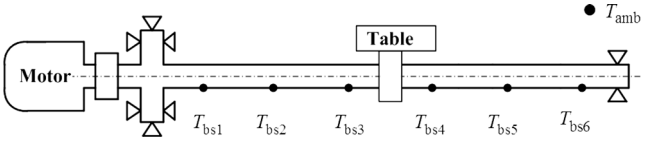

Fig. 1 Temperature measurement points

temperature field of the ball screw system. And the temperature variation of the ball screw system is shown in Fig. 3.

$$T_{\mathrm{bs}} = \frac{1}{6}(T_{\mathrm{bs1}} + T_{\mathrm{bs2}} + T_{\mathrm{bs3}} + T_{\mathrm{bs4}} + T_{\mathrm{bs5}} + T_{\mathrm{bs6}}) \quad (1)$$

Figure 4 shows the X-axis positioning error curves under different temperature conditions. It can be seen from Fig. 4 that each error curve varies little in shape, but the slope differs under different temperature conditions. Besides, the thermally induced error, i.e., the proportion of positioning error after subtracting the initial geometric error, is approximately proportional to the axial position. So, it indicates that the thermal expansion of each measurement interval is approximately the same; it is consistent with the temperature distribution of the ball screw system as introduced above.

3 Thermal analysis of the ball screw system

3.1 Thermal characterization of the ball screw system

It is well known that if a measurement of the ball screw temperature field can somehow be obtained, the corresponding thermal deformation can be calculated. However, it is difficult to measure the ball screw temperature directly owing to the circulating nut. So, numerical forecasting of the ball screw temperature field is a promising alternative way for this study. In this research, as a combined study of the temperature variation and thermal deformation of the ball screw system, the ball screw temperature field is analyzed with FEM based on the following assumptions [22]:

1. The ball screw shaft is a solid cylinder.
2. The friction heat generation rates from the moving nut, the supporting bearings, and the motor are constant under a specific condition.
3. The convection heat transfer coefficient remains constant under a specific condition.
4. The radiation heat is not significant that could be neglected.

Figure 5 shows the FEM schematic diagram for a ball screw shaft. There are mainly three internal heat sources during the warm-up phase, including friction heat from the moving nut q_{nut}, friction heat from the front supporting bearing and the motor q_{b1}, and friction heat from the rear supporting bearing q_{b2}. In addition, a part of the generated heat is dissipated to the ambient air via forced convection q_{h}, and the heat convection rate is proportional to the temperature difference between the ball screw and the ambient air. The

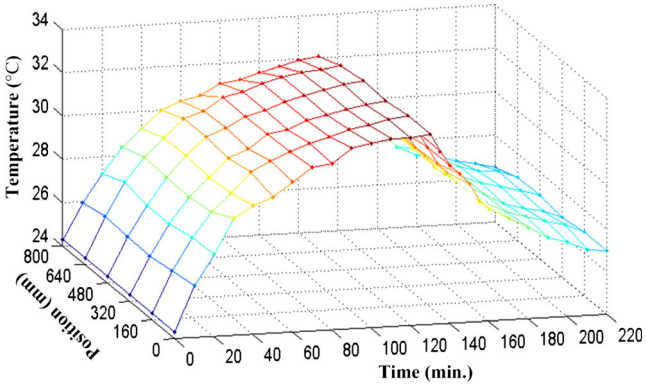

Fig. 2 Temperature data of the six measurement points on the ball screw

transient-state thermal characteristic of the ball screw during the warm-up phase is expressed as follows:

$$q_{\mathrm{nut}} + q_{\mathrm{b1}} + q_{\mathrm{b2}} - h_{\mathrm{w}}A(T_{\mathrm{bs}} - T_{\mathrm{amb}}) = \rho c V \frac{\partial T_{\mathrm{bs}}}{\partial t} \quad (2)$$

$$\Delta T_{\mathrm{bs}} = T_{\mathrm{bs}} - T_{\mathrm{amb}} \quad (3)$$

where A and V are the flank surface area and volume, respectively; h_{w} is the forced convection heat transfer coefficient; ρ is the material density; c is the specific heat; t is the warm-up time; and ΔT_{bs} denotes the temperature difference between the ball screw and the ambient air.

It can be seen from Fig. 3 that the ball screw temperature shows a stable exponential rise state during the warm-up phase. It increases sharply in the initial warm-up phase and gradually slows down until a steady state. The exponential rise is due to the fact that the heat convection rate is related to the temperature difference between the ball screw and the ambient air. The larger the temperature difference is, the higher the heat convection rate becomes. Therefore, as the ball screw temperature rises constantly with warm-up time, the heat convection rate would accelerate progressively while the friction heat generation rate remains constant, so the ball screw temperature variation rate is lowered gradually to a steady state. Consequently, an exponential growth

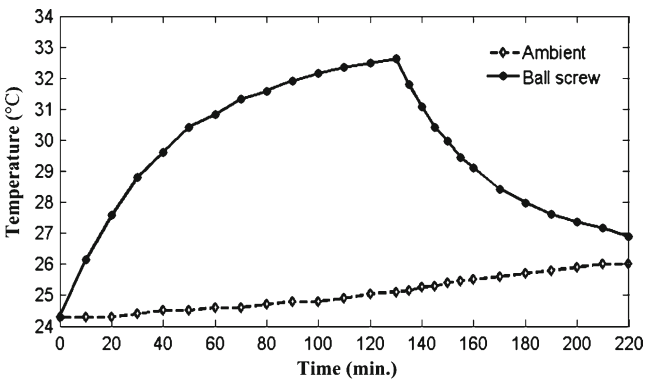

Fig. 3 Temperature variation of the ball screw system

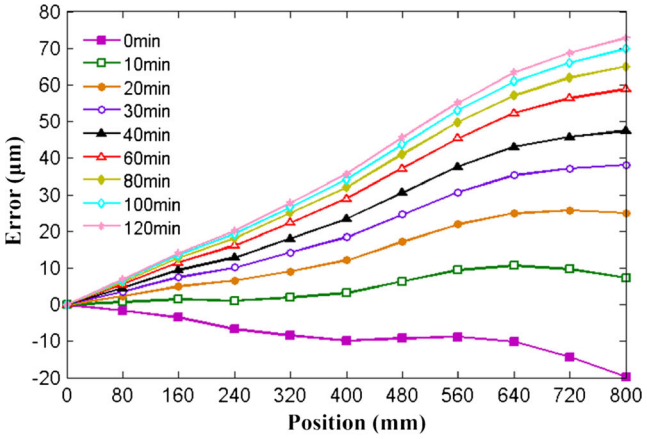

(a) Warm-up phase

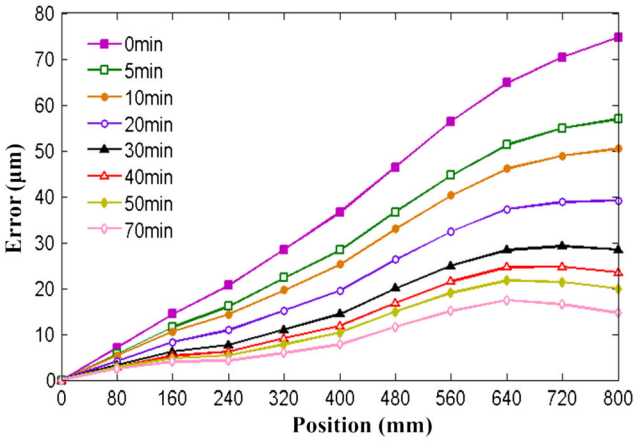

(b) Natural cooldown phase

Fig. 4 *X*-axis positioning errors under different temperature conditions

model is defined to describe the temperature characteristic of the ball screw during the warm-up phase.

$$T_{bs} = T_{amb} + \Delta T_{bs}(\max)\cdot\left(1-e^{-t/\tau_w}\right) \tag{4}$$

where $\Delta T_{bs}(\max)$ is the steady value of ΔT_{bs} under the thermal equilibrium state and τ_w is the exponential time constant during the warm-up phase.

There exist two thermal boundary states for the ball screw system during the warm-up phase:

1. Thermal equilibrium state

   Under the thermal equilibrium state, the convection heat is consistent with the friction heat. So, no more accumulated heat would be added to the ball screw system, and the ball screw temperature would remain constant, expressed as follows:

$$\lim_{t\to\infty}\frac{\partial T_{bs}}{\partial t} = 0 \tag{5}$$

   Substituting Eqs. (4) and (5) into Eq. (2), the total friction heat can be derived as follows:

$$q_{in} = q_{nut} + q_{b1} + q_{b2} = h_w A \Delta T_{bs}(\max) \tag{6}$$

where q_{in} is the total friction heat.

2. Thermal initial state

   Under the initial state, the internal heat sources are eliminated for a long time, and the ball screw temperature field is almost consistent with the ambient temperature, expressed as follows:

$$\lim_{t\to 0}\Delta T_{bs} = T_{bs} - T_{amb} = 0 \tag{7}$$

   Substituting Eqs. (4), (6), and (7) into Eq. (2), the time constant τ_w can be derived as follows:

$$\tau_w = \frac{\rho c d}{4h_w} \tag{8}$$

where d is the diameter of the ball screw.

During the natural cooldown phase, the friction heat generation stops, and the previously accumulated friction heat would be gradually dissipated to the ambient air via natural convection. The transient-state thermal characteristic of the ball screw during the natural cooldown phase is expressed as follows:

$$-h_c A(T_{bs} - T_{amb}) = \rho c V\frac{\partial T_{bs}}{\partial t} \tag{9}$$

where h_c is the natural convection heat transfer coefficient.

It can be seen from Fig. 3 that the ball screw temperature also shows a stable exponential decrease during the cooldown phase. Similarly, an exponential decrease model is defined to describe the temperature characteristic of the ball screw during the cooldown phase.

$$T_{bs} = T_{amb} + \Delta T_{bs}(\text{int})\cdot e^{-t/\tau_c} \tag{10}$$

where $\Delta T_{bs}(\text{int})$ is the initial value of ΔT_{bs} when the feed system is stopped and τ_c is the exponential time constant during the cooldown phase.

Similarly, the time constant τ_c can be derived by substituting Eq. (10) into Eq. (9), considering the

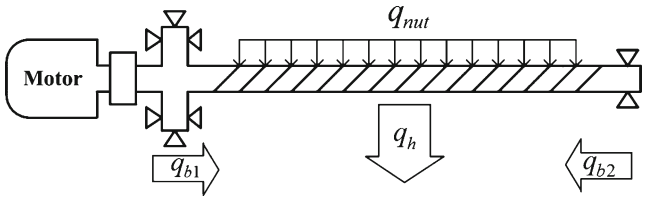

Fig. 5 Finite element model

thermal initial boundary state during the cooldown phase $\lim_{t\to 0}\Delta T_{bs} = T_{bs} - T_{amb} = \Delta T_{bs}(\text{int})$

$$\tau_c = \frac{\rho c d}{4h_c} \tag{11}$$

3.2 Identification of the thermal boundary conditions

To identify the thermal analysis above, the measured temperature data of Fig. 3 is fitted using the exponential growth model as defined in Eq. (4), and the result is shown as follows:

$$\Delta T_{bs} = T_{bs} - T_{amb} = 7.6\left(1 - e^{-t/2170}\right) \tag{12}$$

Figure 6 shows the fitting result of the ball screw temperature during the warm-up phase. It can be seen from Fig. 6 that the fitted curve could match quite well with the measured value. Comparing Eq. (4) with Eq. (12), $\Delta T_{bs}(\max)$ and τ_w can be obtained as $\Delta T_{bs}(\max)$=7.6 °C, τ_w=2,170 s.

Substituting $\Delta T_{bs}(\max)$ and τ_w into Eqs. (6) and (8), the forced convection heat transfer coefficient h_w and the total friction heat q_{in} can be calculated as

$$\begin{aligned} h_w &= \frac{\rho c d}{4\tau_w} = 16.2\ \text{w/m}^2.^{\circ}C \\ q_{in} &= q_{nut} + q_{b2} + q_{b2} = h_w A \Delta T_{bs}(\max) = 13.9\ \text{w} \end{aligned} \tag{13}$$

where material density ρ is 7.85×10^3 kg/m^3, specific heat c is J/Kg.°C.

Similarly, the exponential decrease model defined in Eq. (10) is used to fit the temperature data during the cooldown phase, and the result is shown as follows:

$$\Delta T_{bs} = T_{bs} - T_{amb} = 7.6e^{-t/2470} \tag{14}$$

Figure 6 also shows the fitting result of the ball screw temperature during the natural cooldown phase. It can be seen from Fig. 6 that the fitted curve could also match quite well with the measured value during the cooldown phase. So, the exponential growth and decrease models can be well used to predict the ball screw temperature variation. Comparing Eq. (10) with Eq. (14), $\Delta T_{bs}(\text{int})$ and τ_c can be obtained as $\Delta T_{bs}(\text{int})$=7.6 °C, τ_c=2,470 s.

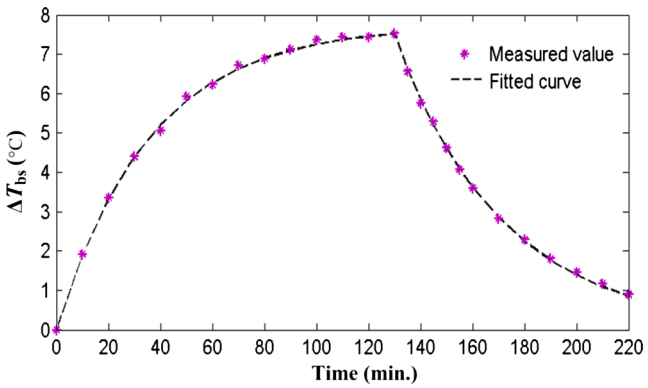

Fig. 6 Fitting curves of ΔT_{bs} during the warm-up and cooldown phases

Substituting τ_c into Eq. (11), the natural convection heat transfer coefficient h_c can be calculated as

$$h_c = \frac{\rho c d}{4\tau_c} = 14.2\ \text{w/m}^2.^{\circ}C \tag{15}$$

According to the thermal boundary conditions identified above, a finite element model was built for the X-axis ball screw as shown in Fig. 7. It was found that when q_{nut} accounted for 80 % of the total friction heat, i.e., q_{nut} was 11.12 w while q_{b1} and q_{b2} were 1.68 and 1.1 w, respectively, the simulation (as shown in Fig. 7) matched quite well with the experimental result. It can be seen from the simulation that the ball screw shaft surface has an almost uniform temperature distribution after a 130-min warm-up, and the maximum temperature increases by 7.8 °C with respect to the ambient temperature; it is in good agreement with the experimental result. So, the thermal boundary conditions identified above is quite accurate and can be used in the actual application.

3.3 Thermal characteristics of the ball screw under various feed rates

To identify the influence of feed rate on the ball screw temperature field, additional experiments were conducted to study the ball screw thermal behaviors under various feed rates. Figure 8 shows the ball screw temperature variation under the feed rate of 5, 8, and 10 m/min, respectively.

It can be seen from Fig. 8 that the steady value of ΔT_{bs} would increase with the feed rate; while the temperature variation pattern is similar in each case, it

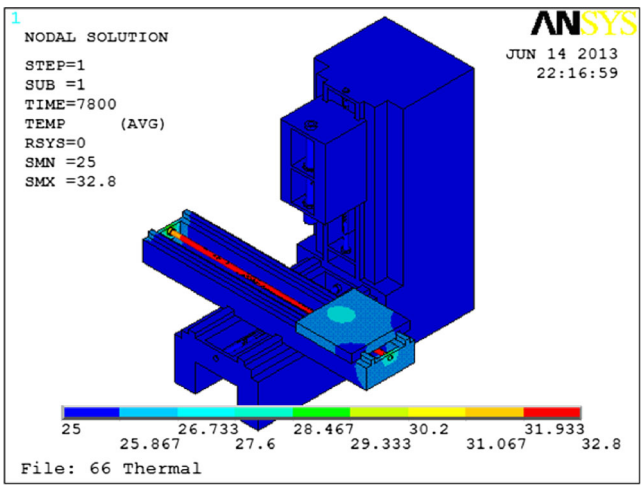

Fig. 7 Temperature distribution of the X-axis ball screw after a 130-min warm-up

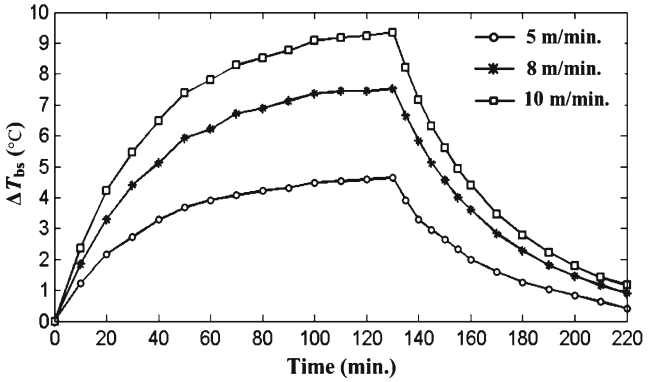

Fig. 8 Variation of ΔT_{bs} under different feed rates

always shows a stable exponential rise state under different feed rates. Besides, it was also found that the friction heat generated during the warm-up phase increased with feed rate in a linear pattern, and the exponential time constant τ_c remained almost constant under different ΔT_{bs}(int). Therefore, the exponential models presented above can be well used to predict the ball screw temperature variation under different operating conditions, and the steady value needs to be adjusted according to the feed rate.

4 Modeling for positioning error

As shown in Fig. 4, positioning error is a quasi-static error; it is not only related to the position coordinate but also affected by the temperature field of the ball screw system. There are mainly two types of heat sources for the ball screw systems: internal heat sources and external heat sources. The former mainly include friction heat from the moving nut, the supporting bearings, and the motor, and the latter mainly refer to the ambient temperature variation. Therefore, according to its original error sources, positioning error can be divided into initial geometric error and thermal errors caused by internal and external heat, respectively.

Additionally, it is found from Fig. 4 that the slope of the positioning error curves increases constantly with the temperature in a linear pattern, but the error curve varies little in shape. So, the comprehensive positioning error model can be expressed as follows:

$$\mathrm{Er}(x,T) = \mathrm{Er_g}(x) + \mathrm{Er_T}(x) = \mathrm{Er_g}(x) + k_T \cdot x \tag{16}$$

Where $\mathrm{Er}(x,T)$ is the total positioning error, $\mathrm{Er_g}(x)$ is the initial geometric error, $\mathrm{Er_T}(x)$ is the thermally induced error, k_T is the curve slope variation with respect to the initial geometric error curve, and x is the nominal position of X-axis.

Each term is defined as follows:

$$\mathrm{Er_g}(x) = \sum_{i=0}^{n} a_i \cdot x^i = a_0 + a_1 x + a_2 x^2 + \cdots + a_n x^n \tag{17}$$

$$k_T = k_{bs}\Delta T_{bs} + k_{amb}\Delta T_{amb} \tag{18}$$

$$\Delta T_{amb} = T_{amb} - T_{amb}(\mathrm{int}) \tag{19}$$

where a_i is the coefficient for the polynomials; k_{bs} and k_{amb} are the thermal expansion coefficients for internal and external heat, respectively; and T_{amb}(int) is the reference temperature when the initial geometric error was measured.

The initial geometric error $\mathrm{Er_g}(x)$ is the basic error curve measured at the reference temperature. It is only related to the position coordinate, so it could be modeled with polynomial regression as above. The thermally induced error is determined by the temperature and position coordinate, and the robustness of the thermal error model is a key factor determining whether the compensation is practical or not. Therefore, to improve the robustness of the comprehensive error model and reduce the affection of ambient temperature variation, the thermal effects caused by internal and external heat sources are modeled separately here.

The coefficients a_i, k_{bs}, and k_{amb} are derived through the least squares estimation criteria based on the experimental data sets shown in Fig. 4 and Tables 2 and 3. The obtained prediction model for the X-axis positioning error is expressed as follows:

$$\mathrm{Er}(x,T) = \mathrm{Er_g}(x) + k_T \cdot x = \left(0.05 - 0.0089_1 x - 1.78E^{-4}x^2 + 5.14E^{-7}x^3 - 3.40E^{-10}x^4\right) + \left(0.0147\Delta T_{bs} + 0.0117\Delta T_{amb}\right)\cdot x \tag{20}$$

Figure 9 shows the modeling results for the X-axis positioning error during the warm-up and natural cooldown phases. It can be seen from Fig. 9 that the fitted curves could match quite well with the actual measured error, and the modeling accuracy turns out to be quite satisfactory. So, when the ball screw temperature field is derived using the numerical forecasting method in Section 3, the corresponding thermal deformation can also be predicted with high accuracy.

Table 2 k_T variation during the warm-up phase

Warm-up time (min)	Curve slope (k_T)	Temperature variation (°C)	
		ΔT_{bs}	ΔT_{amb}
0	0	0	0
10	0.033	1.92	0
20	0.055	3.36	0
30	0.071	4.40	0.10
40	0.083	5.06	0.20
60	0.098	6.22	0.30
80	0.105	6.88	0.40
100	0.111	7.36	0.50
120	0.115	7.44	0.75

5 Compensation implementation and results

5.1 Framework of the compensation system

The real-time compensation system developed in this paper consists of hardware platform and compensation software, and the schematic diagram of the compensation system is illustrated in Fig. 10. The hardware platform is composed of wireless temperature acquisition unit and a compensation controller. The compensation controller is realized on an industrial microcomputer, and it is integrated with a Fanuc 31i CNC (computer numerical control) system through the embedded Ethernet interface; the mutual data interaction is achieved based on the Fanuc Ethernet data transmission protocol. Fast Ethernet data interaction of 100 Mbps is supported by the Fanuc 31i CNC system as a standard function, and it has been tested that one compensation cycle could be completed in 8 ms or less; therefore, it could surely meet the real-time compensation requirement of the quasi-static thermal errors in the machining process.

The compensation software is mainly composed of two modules: ball screw temperature prediction module and real-time compensation module. The temperature prediction module is used to predict the temperature variation of the ball screw according to the FEM-based exponential models, and the prediction process is as follows:

1. According to the thermal boundary conditions identified in Section 3, finite element models are preestablished to simulate the ball screw temperature field under different feed rates.
2. According to the simulation and experimental results, exponential growth model (Eq. (4)) is established to fit the ball screw temperature during the warm-up phase, and the steady value is updated according to the feed rate. Similarly, exponential decrease model (Eq. (10)) is established for the cooldown phase.
3. The exponential growth model (Eq. (4)) is used to predict the ball screw temperature variation ΔT_{bs} in real time during the warm-up phase, and the feed rate and warm-up time are taken as inputs. Similarly, the exponential decrease model (Eq. (10)) is used for temperature prediction during the cooldown phase.

Table 3 k_T variation during the cooldown phase

Cooldown time (min)	Curve slope (k_T)	Temperature variation (°C)	
		ΔT_{bs}	ΔT_{amb}
0	0.117	7.52	0.80
5	0.106	6.56	0.85
10	0.096	5.76	0.95
20	0.080	4.62	1.10
30	0.068	3.60	1.20
40	0.061	2.83	1.30
50	0.054	2.29	1.40
70	0.046	1.46	1.60

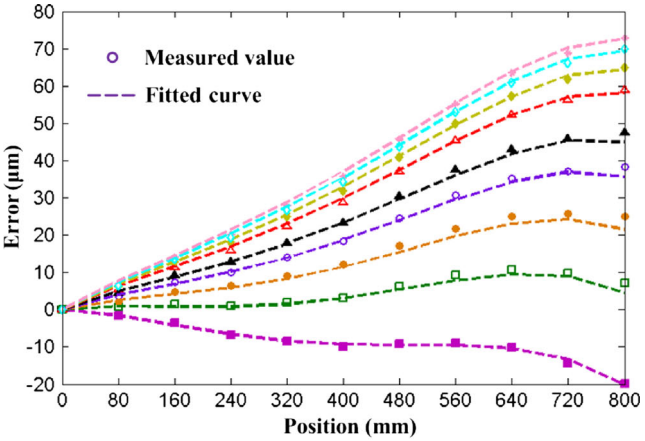

(a) Warm-up phase

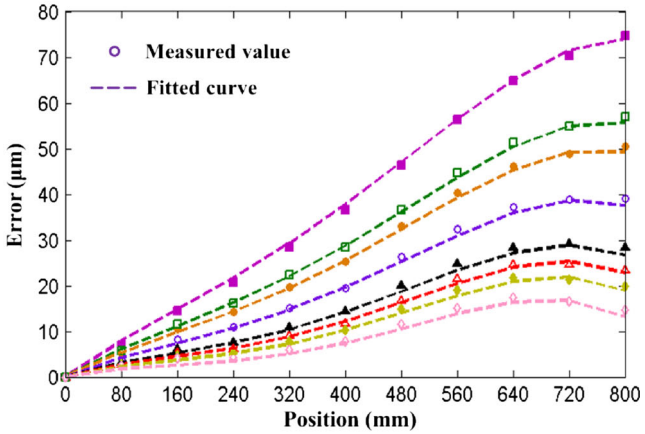

(b) Natural cooldown phase

Fig. 9 Fitting results of error modeling under different temperature conditions

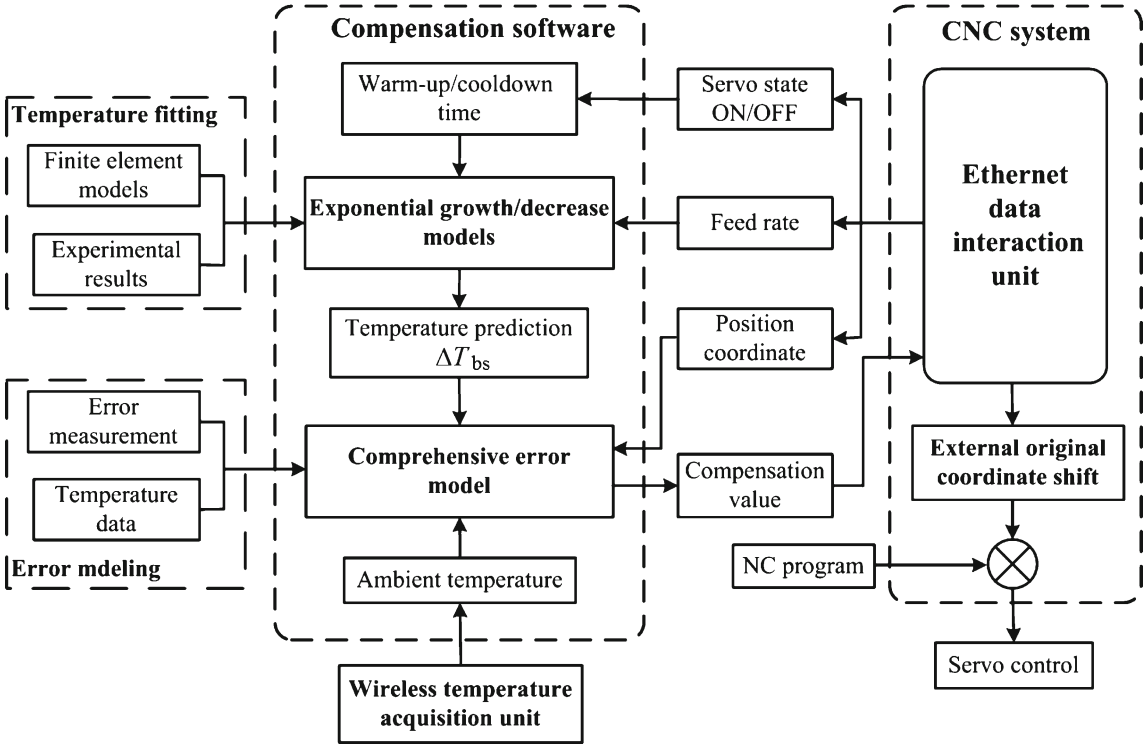

Fig. 10 Real-time error compensation system

The compensation module is used to calculate the real-time positioning error of the machine tool and send the compensation signals to the CNC system. The compensation process is as follows:

1. Reading the real-time machine coordinate through the Ethernet data interaction unit.
2. Obtaining the real-time temperature variation of the ball screw (ΔT_{bs}) from the temperature prediction module and reading the ambient temperature from the wireless temperature acquisition unit
3. Calculation of the real-time positioning error according to the comprehensive error model elaborated in Eq. (20)
4. Transmission of the calculated compensation value to the CNC system in real time through the Ethernet data interaction unit

Then, the compensation function is achieved in the CNC system based on the function of external machine original coordinate shift. The CNC system adds these compensation signals to modify the motion command of the servo control system by shifting the origin of the machine coordinate, and the cutting tool is moved with respect to the workpiece in the opposite direction. This compensation method is quite convenient in the actual implementation, as it has no interference with the original machining program.

5.2 Compensation results

To validate the effectiveness of the proposed modeling algorithm and the feasibility of the compensation method, a series of compensation experiments were conducted on the machining center under different experimental conditions. The overall experimental procedure is listed as follows:

1. Measured the *X*-axis positioning error under the initial state with and without compensation, respectively
2. Warmed up the machine tool with a feed rate of 5 m/min for 30 min and measured the positioning error with and without compensation, respectively
3. Warmed up the machine tool continuously with a different feed rate of 8 m/min for another 30 min and measured the positioning error with and without compensation, respectively
4. Stopped the machine tool for natural cooldown and measured the positioning error with and without compensation, respectively, after 20 min

Figure 11 shows the compensation results for the *X*-axis positioning error under different temperature conditions. It can be seen from Fig. 11 that the maximum initial geometric error was reduced from −16 to 2.5 μm after compensation. Additionally, the maximum positioning error increased from −16 to 21.4 μm after warming up the machine tool for the first 30 min

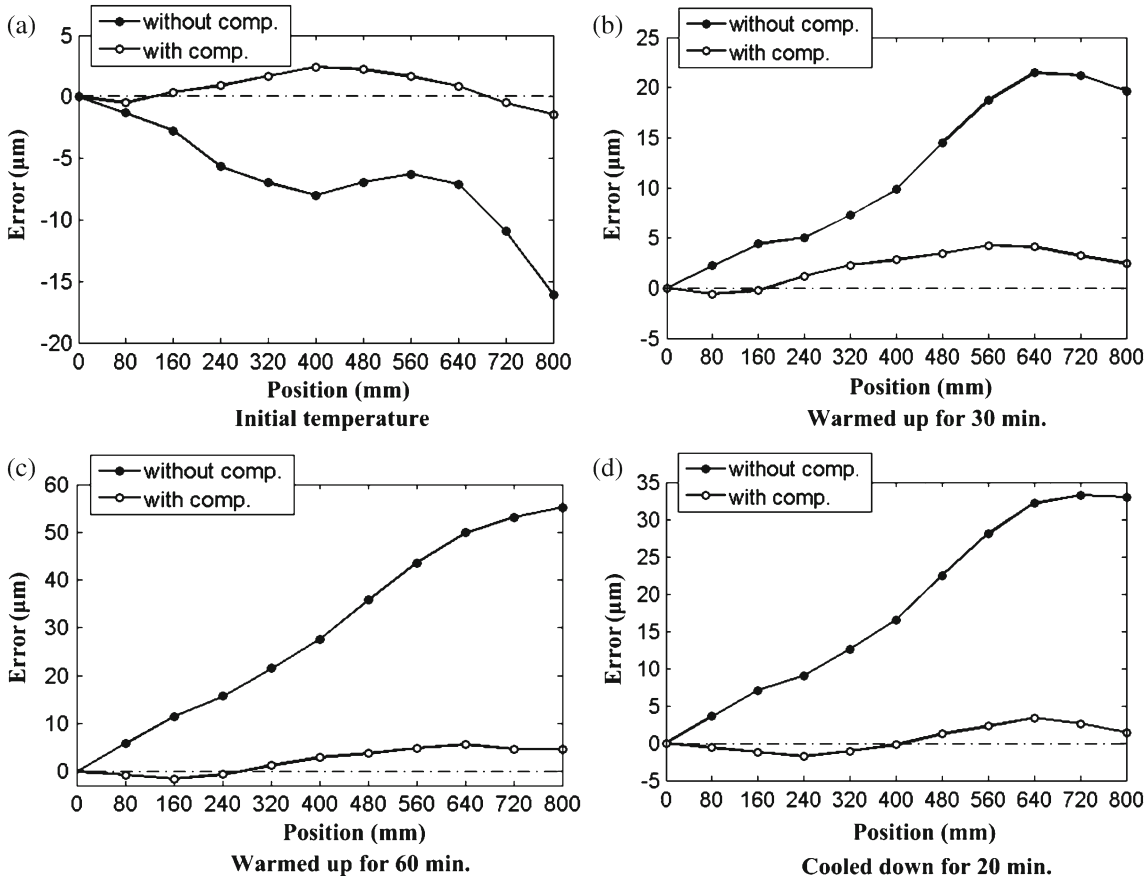

Fig. 11 Compensation results under different experimental conditions

and rose to 55.1 μm after another 30-min warm-up with a higher feed rate. Thereafter, the maximum positioning error decreased to 33.2 μm after a 20-min cooldown. So, it can be seen that the machine tool positioning error shows a time-varying characteristic with the temperature, and the thermally induced positioning error has a significant effect on the positioning accuracy of machine tools. However, after compensation, the maximum thermal positioning errors during both the warm-up and cooldown phases were reduced to less than 5.6 μm, and the positioning accuracy of the machine tool could be improved by at least 75 % under various temperature conditions. Consequently, the positioning accuracy of the machine tool could be significantly improved with the implementation of the real-time compensation system.

6 Conclusions

This paper provides a comprehensive error compensation method for the time-varying positioning error of machine tools based on simulation and experimental analysis, and the experimental results showed that the positioning accuracy of the machine tool was significantly improved with the implementation of the real-time compensation system. The following conclusions can be drawn:

1. The FEM-based exponential growth and decrease models proposed in this paper can be used to predict the ball screw temperature variation with high accuracy. Additionally, combined with the experimental results, they can also be used to identify the actual thermal boundary conditions of the ball screw system.
2. Through the direct thermal analysis of the ball screw temperature field during both the warm-up and cooldown phases and considering the thermal effects caused by internal and external heat, respectively, the comprehensive error model established in this paper could achieve a better compensation performance in terms of accuracy and robustness.

3.Real-time error compensation is achieved on the Fanuc 31i CNC system based on the function of external machine original coordinate shift and fast Ethernet data interaction. One compensation cycle is completed in just 8 ms with the fast Ethernet data interaction through the embedded Ethernet interface. Moreover, this compensation method is quite convenient in the actual implementation, as it has no interference with the original machining program.

Acknowledgments This work was funded by the National Science Foundation Project of the People's Republic of China (no. 51275305), the Specialized Research Fund for the Doctoral Program of Higher Education (no. 20110073110041), and the Chinese National Science and Technology Key Special Projects (no. 2011ZX04015-031).

References

1. Ramesh R, Mannan MA, Poo AN (2000) Error compensation in machine tools—a review: part II: thermal errors. Int J Mach Tools Manuf 40:1257–1284
2. Bryan J (1990) International status of thermal error research. CIRP Ann Manuf Technol 39:645–656
3. Ni J (1997) CNC machine accuracy enhancement through real-time error compensation. J Manuf Sci Eng ASME 119:717–725
4. Xu ZZ, Liu XJ, Kim HK, Shin JH, Lyu SK (2011) Thermal error forecast and performance evaluation for an air-cooling ball screw system. Int J Mach Tools Manuf 51:605–611
5. Jiang SY, Mao HB (2010) Investigation of variable optimum preload for a machine tool spindle. Int J Mach Tools Manuf 50:19–28
6. Tseng PC, Ho JL (2002) A study of high-precision CNC lathe thermal errors and compensation. Int J Adv Manuf Technol 19:850–858
7. Yang JG, Yuan JX, Ni J (1999) Thermal error mode analysis and robust modeling for error compensation on a CNC turning center. Int J Mach Tools Manuf 39:1367–1381
8. Wu CW, Tang CH, Chang CF, Shiao YS (2012) Thermal error compensation method for machine center. Int J Adv Manuf Technol 59:681–689
9. Wang W, Zhang Y, Yang JG, Zhang YS, Yuan F (2012) Geometric and thermal error compensation for CNC milling machines based on Newton interpolation method. Proc IME C J Mech Eng Sci 227:771–778
10. Yang H, Ni J (2005) Dynamic neural network modeling for nonlinear, nonstationary machine tool thermally induced error. Int J Mach Tools Manuf 45:455–465
11. Mize CD, Ziegert JC (2000) Neural network thermal error compensation of a machining center. Precis Eng 24:338–346
12. Zhang Y, Yang JG, Jiang H (2012) Machine tool thermal error modeling and prediction by grey neural network. Int J Adv Manuf Technol 59:1068–1072
13. Liang RJ, Wenhua Y, Haiyan HZ, Yang Q (2012) The thermal error optimization models for CNC machine tools. Int J Adv Manuf Technol 63:1167–1176
14. Chen JS, Yuan JX, Ni J, Wu SM (1993) Real-time compensation for time-variant volumetric errors on a matching center. J Eng Ind Trans ASME 115:472–479
15. Li YX, Tong HC (2006) Application of time series analysis to thermal error modeling on NC machine tools. J Sichuan Univ 37:74–78
16. Yan JY, Yang JG (2009) Application of synthetic grey correlation theory on thermal point optimization for machine tool thermal error compensation. Int J Adv Manuf Technol 43:1124–1132
17. Li YX, Yang JG, Gelvis T, Li YY (2008) Optimization of measuring points for machine tool thermal error based on grey system theory. Int J Adv Manuf Technol 35:745–750
18. Ramesh R, Mannan MA, Poo AN (2002) Support vector machines model for classification of thermal error in machine tools. Int J Adv Manuf Technol 20:114–120
19. Ko TJ, Gim TW, Ha JY (2003) Particular behavior of spindle thermal deformation by thermal bending. Int J Mach Tools Manuf 43:17–23
20. Kim SK, Cho AW (1997) Real-time estimation of temperature distribution in a ball screw system. Int J Mach Tools Manuf 37:451–464
21. Xia JY, Hu YM, Wu B, Shi TL (2008) Research on the thermal dynamic characteristics and modeling approach of ball screw. Int J Adv Manuf Technol 43:421–430
22. Min X, Jiang S (2011) A thermal model of a ball screw feed drive system for a machine tool. Proc IME C J Mech Eng Sci 225:186–193
23. ISO230-2:2006. Test code for machine tools—part 2: determination of accuracy and repeatability of positioning numerically controlled axes. International Standards Organization
24. ISO230-3:2007. Test code for machine tools—part 3: determination of thermal effects. International Standards Organization